Anal. Chem. **2010,** *82,* 6919–6925

Electrochemical Modulation for Signal Discrimination in Surface Enhanced Raman Scattering (SERS)

Emiliano Cortés,*,† Pablo G. Etchegoin,*,‡ Eric C. Le Ru,‡ Alejandro Fainstein,§ María E. Vela,† and Roberto C. Salvarezza†

Instituto de Investigaciones Fisicoquímicas Teóricas y Aplicadas (INIFTA), Universidad Nacional de La Plata-CONICET, Sucursal 4 Casilla de Correo 16 (1900), La Plata, Argentina, The MacDiarmid Institute for Advanced Materials and Nanotechnology, School of Chemical and Physical Sciences, Victoria University of Wellington, PO Box 600, Wellington, New Zealand, Centro Atómico Bariloche and Instituto Balseiro, Comisión Nacional de Energía Atómica and Universidad Nacional de Cuyo, (8400) San Carlos de Bariloche, Río Negro, Argentina

Electrochemical modulation to induce controlled fluctuations in SERS signals is introduced as a method to discriminate and isolate different contributions to the spectra. The modulation—which can be changed in potential range, amplitude, and frequency—acts as a controllable "switch" to turn on, off, or change specific Raman signals which can then be correlated within the spectra by different fluctuation analysis techniques. Principal component analysis (PCA), either by itself or assisted by fast fourier transform (FFT) prefiltering, are shown to provide viable tools to isolate the different components of the spectra. Electrochemical modulation provides, therefore, a technique to study complex cases of coadsorption, and resolve problems of spectral congestion in SERS signals.

The links between surface-enhanced raman scattering (SERS)[1,2] and electrochemistry go all the way back to the discovery of the effect in the 1970s.[3−5] Since then, electrochemical studies have provided invaluable information on the details of the electronic interaction of molecules with the underlying metal substrate responsible for the SERS enhancement. Particularly important have been studies where the origin of the so-called "chemical enhancement"[6,7] in SERS can be discerned. From a more modern point of view, SERS and electrochemistry have diversified into a myriad of different areas that include the studies of coadsorption (multiple species), biological redox system,[8,9] corrosion, surface science,[10] fuel cells, electrocatalysis, electronic models for charge-transfer processes on surfaces,[11−16] and single-molecule or single hot-spot SERS,[17,18] to name only a few.[19,20] The simultaneous presence of the laser field with electric potentials and/or currents in the many different experimental configurations of substrates with simple, multiple, or tip-like electrodes, together with the variety of environmental variables (like pH or the exact nature of the electrolyte) produce the vast diversity of experimental situations found in the modern applications of SERS to electrochemistry. Tian and co-workers[20] provide a lucid summary of recent advances in SERS for electrochemical applications. It is argued in ref 20 in fact, that electrochemical systems are among the most complex one can study in SERS. The combination of electrochemical processes at interfaces with SERS make these systems particularly challenging, but undoubtedly very relevant to understand fundamental aspects in real analytical and bioanalytical applications. Last, but not least, there are several techniques under development in SERS that combine the basic elements of electrochemical experiments, even though they would not be strictly speaking considered as such. Examples of the latter are recent attempts to combine SERS and molecule transport proper-

* To whom correspondence should be addressed. E-mail: emilianocll@gmail.com (E.C.), pablo.etchegoin@vuw.ac.nz (P.G.E.).

† Universidad Nacional de La Plata-CONICET.

‡ Victoria University of Wellington.

§ Comisión Nacional de Energía Atómica and Universidad Nacional de Cuyo.

(1) Le Ru, E. C.; Etchegoin, P. G. *Principles of Surface Enhanced Raman Spectroscopy and Related Plasmonic Effects*; Elsevier: Amsterdam, 2009.
(2) Aroca, R. F. *Surface-Enhanced Vibrational Spectroscopy*; John Wiley & Sons: Chichester, 2006.
(3) Fleischmann, M.; Hendra, P. J.; McQuillan, A. J. *Chem. Phys. Lett.* **1974**, *26*, 163–166.
(4) Jeanmaire, D. L.; Van Duyne, R. P. *J. Electroanal. Chem.* **1977**, *84*, 1–20.
(5) Albrecht, M. G.; Creighton, J. A. *J. Am. Chem. Soc.* **1977**, *99*, 5215–5217.
(6) Otto, A. *Surface-Enhanced Raman Scattering: Classical and Chemical Origins*; Springer-Verlag: Berlin, 1984.
(7) Tian, Z. Q. *Faraday Discuss.* **2006**, *132*, 309.
(8) Murgida, D. H.; Hildebrandt, P. *Chem. Soc. Rev.* **2008**, *37*, 937–945.
(9) Hildebrandt, P.; Murgida, D. H. *Bioelectrochemistry* **2002**, *55*, 139.
(10) Cai, W. B.; Ren, B.; Li, X. Q.; She, C. X.; Liu, F. M.; Cai, X. W.; Tian, Z. Q. *Surf. Sci.* **1998**, *406*, 9–22.
(11) Gersten, J. I.; Birke, R. L.; Lombardi, J. R. *Phys. Rev. Lett.* **1979**, *43*, 147–150.
(12) Lombardi, J. R.; Birke, R. L.; Lu, T.; Xu, J. *J. Chem. Phys.* **1986**, *84*, 4174–4180.
(13) Xie, Y.; Wu, D. Y.; Liu, G. K.; Huang, Z. F.; Ren, B.; Yan, J. W.; Yang, Z. L.; Tian, Z. Q. *J. Electroanal. Chem.* **2003**, *554*, 417–425.
(14) Lombardi, J. R.; Birke, R. L. *Acc. Chem. Res.* **2009**, *42*, 734–742.
(15) Tognalli, N.; Fainstein, A.; Bonazzola, C.; Calvo, E. J. *J. Chem. Phys.* **2004**, *120*, 1905.
(16) Tognalli, N.; Scodeller, P.; Flexer, V.; Szamocki, R.; Ricci, A.; Tagliazucchi, M.; Calvo, E. J.; Fainstein, A. *Phys. Chem. Chem. Phys.* **2009**, *11*, 7412.
(17) dos Santos, D. P.; Andrade, G. F. S.; Temperini, M. L. A.; Brolo, A. G. *J. Phys. Chem. C* **2009**, *113*, 17737–17744.
(18) Shegai, T.; Vaskevich, A.; Rubinstein, I.; Haran, G. *J. Am. Chem. Soc.* **2009**, *131*, 14390.
(19) Tian, Z. Q.; Ren, B. *Annu. Rev. Phys. Chem.* **2004**, *55*, 197–229.
(20) Wu, D. Y.; Li, J. F.; Ren, B.; Tian, Z. Q. *Chem. Soc. Rev.* **2008**, *37*, 1025–1041.

10.1021/ac101152t © 2010 American Chemical Society
Published on Web 07/26/2010

ties,[21] or the use of electrostatic fields to control the adsorption/desorption of molecules on SERS substrates according to their cationic/anionic nature in solution.[17,22]

It is perhaps due to the complexity of the systems under study that despite all the accumulated work over the last decades the combination of SERS and electrochemistry is still undergoing methodological and analytical advances as a technique. There is a genuine need to develop both new and more advanced methods and analysis tools to attack the ever increasing complexity of the problems that are being investigated (in particular in bioelectrochemical areas). An early example of the latter is the technique of *potential averaged SERS* developed by Tian and co-workers[23] to address the problem of fast electrochemical processes and SERS monitoring of unstable species on the electrodes. Detection of intermediate species in electrochemical reactions by time-resolved SERS has also been tried by Lombardi et al.[24] A more recent example, on the other hand, is the introduction of local imaging of the electrochemical current by surface-plasmon resonances in ref 25. Many of these new techniques are not directly linked or applied to SERS,[26,27] even though they share the same basic elements; that is, the combination of electrochemistry with a detection technique based on surface plasmon resonances.[1]

This paper aims at a methodological development in the combination of SERS and electrochemistry. As such we shall show some basic examples of the technique we propose. To this end, we borrow ideas from well established techniques of *optical modulation*[28] by using the ability of electrochemistry to turn "on" and "off" Raman signals (by changing the resonance conditions of the reduced or oxidized states), as well as to introduce other (more subtle) spectral changes as a function of the applied potential. Variations in SERS signals with potential have been extensively studied in the literature. A common trait is the observation of changes in the overall intensity of the spectra (as the main consequence of the applied potential) when switching from oxidized to reduced species. As a result, changes in the intensity of the SERS spectra due to the oxidation state have been used as a detection parameter in nanobiosensing,[29] to check the permeability of phospholipid membranes[30] or thiol self-assembled monolayers,[31] and to evaluate integrity and redox behavior in proteins;[32] among others.

SERS provides a tool to monitor electrochemical phenomena at concentration levels (~nanomolars, and below) that cannot be followed either in the voltamperogram or with other techniques. Its sensitivity can, in fact, go routinely all the way down to single molecule levels.[33] But *spectral congestion* is very often cited as a common problem for its use[34,35] as was recently reported (for example) to separate resonances of a target molecule from a surrounding lipid matrix.[36] In the technique developed here, electrochemistry provides an external "switch" wherefrom variations in specific SERS signals can be introduced at will (and with a given periodicity). Fluctuation analysis with methods like principal component analysis (PCA)—either by itself or assisted by Fourier "lock-in" prefiltering (vide infra)—can easily follow from here, thus providing a systematic method to isolate SERS signals from different species along the electrochemical cycle (in the background of many possible, sometimes undesirable, contributions).

Electrochemical modulation and signal discrimination could become a very important tool in areas like bioelectrochemistry, to isolate the signals from different species in redox active sites, in samples where we cannot choose at will the purity or spectral characteristics of all the components. The situation of overlapping peaks—or much larger signals from spurious molecules—can prevent the isolation of the interesting spectra displaying an oxidation/reduction cycle. Therefore, the technique is aimed at applications in this latter case, and it applies particularly well to address cases of *coadsorption*; which is a classic case applicable to the electrochemistry of complex multicomponent systems (like biological systems).

EXPERIMENTAL SECTION

A three-electrode cell with a Ag/AgCl (1 M Cl^-) electrode and a high-area platinum foil as reference and counter electrodes, respectively, was used. The working electrode (see below for further details) is immersed in the electrolyte solution (phosphate buffer, pH 6) and this is placed inside an open electrochemical cell that allows focusing on the substrate with long working distance objectives (×10, ×20, ×50, or ×100) through a water/air interface (see the Supporting Information (SI) for further details). All the potentials reported here are referenced to the Ag/AgCl (1 M Cl^-) electrode. Cyclic voltammetry is performed with a potentiostat with digital data acquisition. The whole assembly is placed on top of a motorized $x-y$ stage for microscopy (to allow exploration and mapping of the electrode) and is used on a BX41 Olympus microscope attached to a Jobin-Yvon LabRam spectrometer. All the experiments performed in this paper are done with the 633 nm line of a HeNe laser with 3 mW at the sample. For samples with "high" concentrations of dyes (for SERS standards) like ~20−40 nM, we are mainly interested in *average* signals over the substrate. Therefore, we typically use for these experiments

(21) Ward, D. R.; Halas, N. J.; Ciszek, J. W.; Tour, J. M.; Wu, Y.; Nordlander, P.; Natelson, D. *Nano Lett.* **2008**, *8*, 919–924.
(22) Lacharmoise, P. D.; Etchegoin, P. G.; Le Ru, E. C. *ACS Nano* **2009**, *3*, 66–72.
(23) Tian, Z. Q.; Li, W. H.; Mao, B. W.; Zou, S. Z.; Gao, J. S. *Appl. Spectrosc.* **1996**, *50*, 1569.
(24) Shi, C.; Zhang, W.; Birke, R. L.; Lombardi, J. R. *J. Phys. Chem.* **1990**, *94*, 4766–4769.
(25) Shan, X.; Patel, U.; Wang, S.; Iglesias, R.; Tao, N. *Science* **2010**, *327*, 1363–1366.
(26) Huang, B.; Yu, F.; Zare, R. N. *Anal. Chem.* **2007**, *79*, 2979–2983.
(27) Wang, S.; Huang, X.; Shan, X.; Foley, K. J.; Tao, N. *Anal. Chem.* **2010**, *82*, 935–941.
(28) Yu, P. Y.; Cardona, M. *Fundamentals of Semiconductors: Physics and Materials Properties*; Springer: Berlin, 2004.
(29) Scodeller, P.; Flexer, V.; Szamocki, R.; Calvo, E. J.; Tognalli, N.; Troiani, H.; Fainstein, A. *J. Am. Chem. Soc.* **2008**, *130*, 12690–12697.
(30) Daza Millone, M. A.; Vela, M. E.; Salvarezza, R. C.; Creczynski-Pasa, T. B.; Tognalli, N. G.; Fainstein, A. *Chem. Phys. Chem.* **2009**, *10*, 1927–1933.
(31) Tognalli, N. G.; Fainstein, A.; Vericat, C.; Vela, M. E.; Salvarezza, R. C. *J. Phys. Chem. C* **2008**, *112*, 3741–3746.
(32) Kranich, A.; Naumann, H.; Molina-Heredia, F. P.; Moore, H. J.; Lee, T. R.; Lecomte, S.; de la Rosa, M. A.; Hildebrandt, P.; Murgida, D. H. *Phys. Chem. Chem. Phys.* **2009**, *11*, 7390–7397.
(33) Etchegoin, P. G.; Van Duyne, R. P. *Phys. Chem. Chem. Phys.* **2008**, *10*, 6079.
(34) Casadio, F.; Leona, M.; Lombardi, J. R.; Van Duyne, R. P. *Acc. Chem. Res.* **2010**, *43*, 782–791.
(35) Golightly, R. S.; Doering, W. E.; Natan, M. J. *ACS nano* **2009**, *3*, 2859–2869.
(36) Nguyen, T. T.; Rembert, K.; Conboy, J. C. *J. Am. Chem. Soc.* **2009**, *131*, 1401–1403.

the ×10 objective, to have a large spot diameter ∼10 μm, and minimize photobleaching effects as much as possible.

Rhodamine 6G (RH6G), nile blue (NB), and crystal violet (CV) were obtained from commercial sources (Aldrich) and mixed at the appropriate concentrations with borohydride-reduced Ag colloids[37] (to avoid a citrate capping layer) and with 20 mM KCl; to induce a slight destabilization and the formation of clusters.[38] For each case reported here, the details about the specific concentrations being used are specified in the captions. RH6G, NB, and CV adsorb to the negatively-charged colloids in this case through electrostatic interactions. The colloidal solution is subsequently drop-casted and dried under a mild heat on a clean Ag foil. Once dried, the colloids stick to the Ag foil by van der Waals forces, and remain attached to it upon reimmersion in the phosphate buffer solution. Several regions with multiple dried clusters of colloids can be easily distinguished in the microscope image on the Ag surface after drying. Hence, the Ag foil with the colloids and the dyes is our working electrode, and also provides the ideal means whereupon SERS enhancements (to observe low dye concentrations) can coexists with the ability to perform electrochemistry on the attached molecules. We checked at much higher concentrations (∼1 mM) that, as far the voltamperogram is concerned, the electrochemistry of the dyes on the colloids is indistinguishable from the one where the dyes are directly attached to the Ag foil itself. Note also that, in all of the experiments performed in this work, the dyes were adsorbed beforehand on the colloids (i.e., the dyes are not dissolved in the electrolyte solution itself).

ELECTROCHEMICAL MODULATION AND SIGNAL ISOLATION

Mixture of NB and RH6G. To fix ideas, we develop the method through an example. Consider the case of a mixture of two classic SERS dyes: RH6G and NB in concentrations of 40 and 20 nM, respectively. We perform cyclic voltammetric runs varying the scan rate (i.e., the period), typically in the range ∼20−100 s per cycle, while monitoring the SERS signal on the electrode simultaneously with a much smaller integration time to follow the dynamics. This gives us the possibility to choose the best scan rate that allows us to follow the dynamics of the system. According also to the choice of the potential window, the different coadsorbed species will be modulated differently. This adds then a second degree of freedom (besides the period of the modulation) to be chosen by the experimentalist: that is, the potential range of the modulation. In the case of Figure 1 we modulated the potential in the range between −50 and −550 mV at a fix scan rate of 50 mV·sec^{-1}. NB will experience oxidation/reduction cycles between these two values, while RH6G will only start to be reduced at a potential of ∼−400 mV and lower.[17] Another important detail is that the electrochemical modulation does not cross at any point the *potential of zero charge* (pzc = −0.9 V) of the electrode,[39] meaning that the dyes (which are positively charged in solution) remain all the time on a positively charged electrode in the entire modulation range. None of the phenomena reported in this paper can be ascribed to adsorption/desorption produced by a change in polarity of the electrode across the pzc point, but rather to oxidation/reduction of the species. Note also that the scan rates used in our experiences are fast enough compared to those reported for "electrostatic guiding".[17,22]

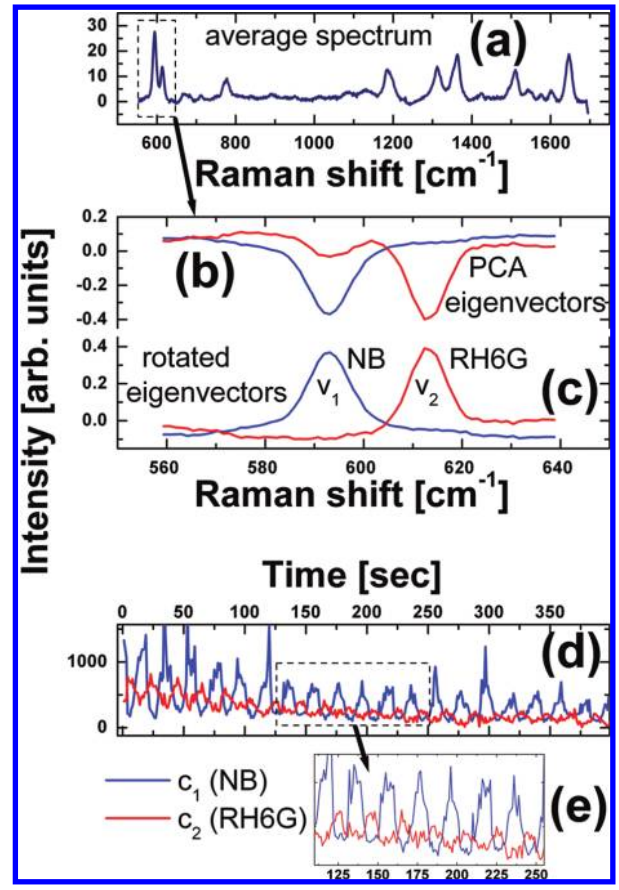

Figure 1. (a) Average spectrum for a sample with 20 nM of NB and 40 nM of RH6G which is modulated electrochemically in the potential range −50 to −550 mV at a scan rate of 50 mV·sec^{-1}. Both signals of NB and RH6G are clearly visible, and both dyes are modulated in different electrochemical potential ranges. The "fingerprint" region containing the 590 cm^{-1} mode of NB and the 610 cm^{-1} one of RH6G (dashed box in (a)) is analyzed by PCA, resulting in the two dominant eigenvectors shown in (b). The spectra in (b) contains a *linear combination* of the two independent spectra of NB and RH6G, which can be obtained by a suitable change of basis (described in full detail in ref 40). The new eigenvectors (obtained from a linear combination of the PCA ones) that describe the two physically independent components (NB and RH6G) are shown in (c). With these eigenvectors we can make a decomposition of the spectra to obtain the two coefficients that describe (for each event) the intensity as a linear combination of v_1 and v_2. These coefficients are shown in (d), with a blown-out region in (e) where the dephasing of the electrochemical modulation of both signals can be observed.

In order to optimize the presentation of the material here without dwelling too much into collateral issues, we present the main details of the basic electrochemistry of NB and RH6G in the SI, as well as the basic aspects of the analysis with principal component analysis (PCA), and PCA with FFT prefiltering.[41,42] As explained in the SI, both analysis techniques (PCA and FFT) are quite widespread, and we shall therefore assume that the

(37) Creighton, J. A.; Blatchford, C. G.; Albrecht, M. G. *J. Chem. Soc., Faraday Trans. 2* **1979**, *75*, 790–798.
(38) Meyer, M.; Le Ru, E. C.; Etchegoin, P. G. *J. Phys. Chem. B* **2006**, *110*, 6040.
(39) Niaura, G.; Gaigalas, A. K.; Vilker, V. L. *J. Phys. Chem. B* **1997**, *101*, 9250–9262.

reader has a basic understanding of them. Hereafter, we shall go directly to the presentation of the main results.

Figure 1(a) shows the average signal over 400 spectra taken with integration time of 1 s, with an electrochemical modulation period of 20 s. The average has clear fingerprint peaks of both dyes; for example the 590 and 610 cm^{-1} modes of NB and RH6G, respectively. The intensity of these peaks is modulated differently in the potential window selected, that is, their redox potentials are different. This is a case nevertheless where both signals of the coadsorbed species are clearly visible, and show in some cases some degree of overlap (like the 1645 and 1650 cm^{-1} modes of NB and RH6G, respectively). We first show an analysis in Figure 1 based on a spectral region that contains fingerprint modes of both dyes, like the region around ~600 cm^{-1} shown in a dashed box in Figure 1(a). A PCA analysis of this region[40] immediately identifies the presence of two main modulated components in the spectra. As explained in the SI though, being a linear decomposition technique, PCA always provides a *linear combination* of the right answer in the form of principal "eigenvector" spectra (in this case the first two of them, shown in Figure 1(b)). In order to go from this two PCA eigenvectors to the real spectra that represent the individual contributions of NB and RH6G, a linear transformation (which we shall call "rotation") of these eigenvectors is required. An entirely equivalent situation occurs with the application of PCA to the analysis of fluctuations from single molecule spectra; as explained in full length in ref 40. The "rotated" eigenvectors obtained in this case are shown in Figure 1(c), and represent the isolated contributions of NB and RH6G to each individual spectrum. Once these two eigenvector spectra (v_1 and v_2 in Figure 1(c)) are known, a standard linear decomposition can be performed on each spectra I_i in the time series ($i = 1, 2, ..., 400$), to represent it as a linear combination (with two coefficients) of the rotated PCA eigenvectors; that is, $I_i = c_1v_1 + c_2v_2$. The values of the coefficients, therefore, represent the particular contribution of NB and RH6G to an individual spectrum, and this is shown explicitly in Figure 1(d). Figure 1(e), in addition, shows a blown-out region of the time evolution of the coefficients where it can be appreciated that the two signals are being modulated differently at different times, accounting for the different intrinsic electrochemical properties of both dyes as a function of the sweeping potential. Note that time evolution can be converted to potential, since we know exactly the period of electrochemical modulation applied externally. An example of this is shown in the SI. The coefficients in Figure 1(d) and (e) are obviously in arbitrary units, since the Raman intensity itself is in arbitrary units too. What matters is not the absolute units, but rather the relative values of the coefficients representing the particular contributions to the total coming from the different electrochemical species.

Therefore, Figure 1 demonstrates clearly that the combination of electrochemical modulation with PCA analysis can (i) resolve the problem of spectral congestion, and (ii) identify in addition the ranges of electrochemical potentials where the different species experience their modulation. This is emphasized in Figure 1(e), where the "dephasing" of the coefficients c_1 and c_2 representing the relative contributions of NB and RH6G, respectively, can be easily seen. The fact that RH6G only starts to be reduced toward the lowest negative range of the potential ($E < -400$ mV) appears as a "dephasing" of the coefficients in time, while the successive electrochemical cycles evolve. Figure 1(d) also shows a slight reduction in the amplitude of the coefficients produced by photobleaching at the observation point. It may also have partial contribution from natural long-term desorption of the dyes into the buffer. Photobleaching, in general, tends to be one of the major limiting factors to obtain unlimited sampling of the signal.

Moving on from the simplest case in Figure 1, if we want to carry out the analysis over the entire spectral range (rather than a small window with fingerprint modes, like in Figure 1), special care must be taken with background contributions. Backgrounds are in general problematic in SERS[43] and, unlike the Raman peaks themselves, they can have a variety of origins (including molecules that are not in contact with the electrode). Furthermore, there will be in general a correlation between the background and the Raman signal created by the dispersion of the plasmon resonances producing SERS.[43−45] Here, we want to concentrate in a first approximation only on the Raman signals themselves and, therefore, the background will be removed[46] to avoid its presence in the PCA analysis. This should be done with care and the results should be assessed on a case-by-case basis. Backgrounds in SERS can be particularly problematic in the single molecule limit, where the dispersion of an individual plasmon resonance at a hot-spot can be revealed.[43,47] Measuring an average over many molecules is in a way an advantage, for differing types of backgrounds tend to average out and we are left with a case of background contribution that is easier to subtract. The background of each individual spectrum is subtracted with a wavelet transform that is fully described in ref 46 (including the program which is freely available[46]). The success of the background subtraction procedure to deconvolute the spectra is judged here by the ability of the PCA analysis to distinguish the two main contributions to the signal in the full spectral range (which are known in this case).

Effectively, Figure 2 shows the equivalent analysis of Figure 1 in the full spectral range. Once the backgrounds are subtracted, and the two main PCA eigenvector spectra rotated, we recover the independent spectra of NB and RH6G from the mixture. Except for a few minor imperfections, the separation of the spectral components is almost perfect, and can be also distinguished in terms of the respective electrochemical modulation ranges for the potential. As in Figures 1(d) and (e), the dephasing of the coefficients from the contributions of NB and RH6G, according to the different values of the redox potentials over the cyclic voltammetry runs, can be clearly observed again in Figure 2(d). It is particularly worth emphasizing that the spectral deconvolution

(40) Etchegoin, P. G.; Meyer, M.; Blackie, E.; Le Ru, E. C. *Anal. Chem.* **2007**, *79*, 8411.
(41) Jolliffe, I. T. *Principal Component Analysis*; Springer Verlag:Berlin, 2002.
(42) Hyvrinen, A.; Karhunen, J.; Oja, E. *Independent Component Analysis*; John Wiley & Sons: New York, 2001.
(43) Buchanan, S.; Le Ru, E. C.; Etchegoin, P. G. *Phys. Chem. Chem. Phys.* **2009**, *11*, 7406.
(44) Le Ru, E. C.; Etchegoin, P. G.; Grand, J.; Felidj, N.; Aubard, J.; Levi, G.; Hohenau, A.; Krenn, J. R. *Curr. Appl. Phys.* **2008**, *8*, 467.
(45) Le Ru, E. C.; Grand, J.; Felidj, N.; Aubard, J.; Levi, G.; Hohenau, A.; Krenn, J. R.; Blackie, E.; Etchegoin, P. G. *J. Phys. Chem. C* **2008**, *112*, 8117.
(46) Galloway, C.; Le Ru, E. C.; Etchegoin, P. G. *Appl. Spectrosc.* **2009**, *63*, 1371.
(47) Itoh, T.; Yoshida, K.; Biju, V.; Kikkawa, Y.; Ishikawa, M.; Ozaki, Y. *Phys. Rev. B* **2007**, *76*, 085405.

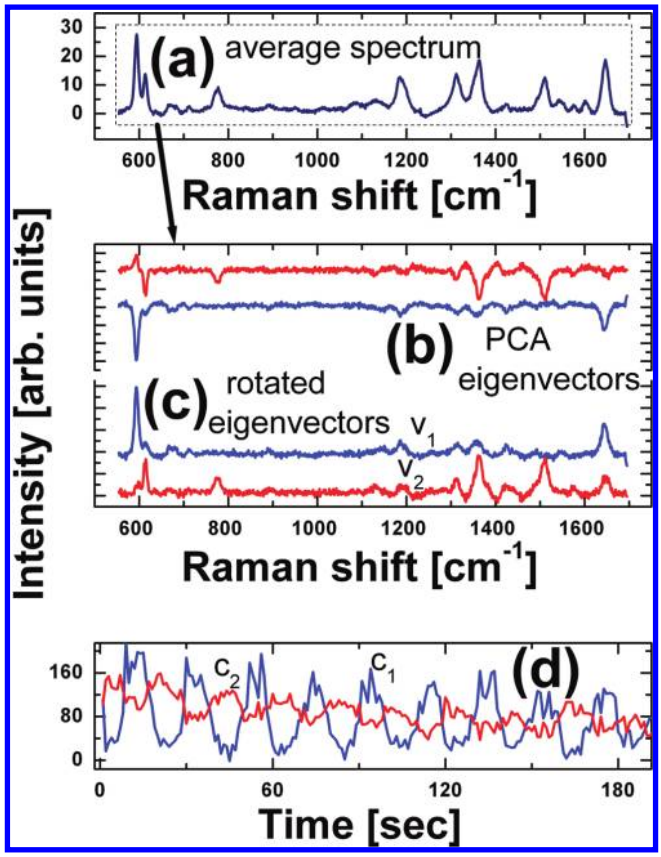

Figure 2. With a suitable removal of the background[46] for all events, the full spectra of NB and RH6G can be deconvoluted again from the modulated time series through PCA. The region analyzed now is the full spectral window shown in (a) (dashed line). The two main eigenvectors and the "rotated" ones[40] (representing the independent contributions of NB and RH6G) are shown in (b) and (c), respectively. The spectra of two compounds can be deconvoluted, and their time (or potential) dependence followed through the time evolution of the two coefficients in (d), that describe each event as a linear combination of v_1 and v_2 in (c). The dephasing of the electrochemical modulation of the two compounds can again be appreciated in (d).

through the electrochemical modulation works very well even in regions where a substantial overlap of peaks occurs. An example of the latter is shown in Figure 3, for the region around ~1650 cm^{-1}, which has contributions from breathing modes of both NB and RH6G (but at slightly different frequencies). As can be appreciated from Figure 3, the different modulation induced through the electrochemical cycle on both compounds is good enough to "deconvolute" closely laying peaks within their natural widths.

Mixture of NB and CV. All in all, the case presented in the previous section represents a relative "easy" case of spectral deconvolution for PCA with electrochemical modulation; starting from the fact that both compounds have comparable contributions to the intensity of the spectra and can be easily identified in terms of their contributions to fluctuations (which is the whole basis of PCA[41,42]). A substantially more challenging case is to try recover a small signal from a background of other contributions to the spectra (that might be unavoidable in many real cases). We treat this case here also with an example.

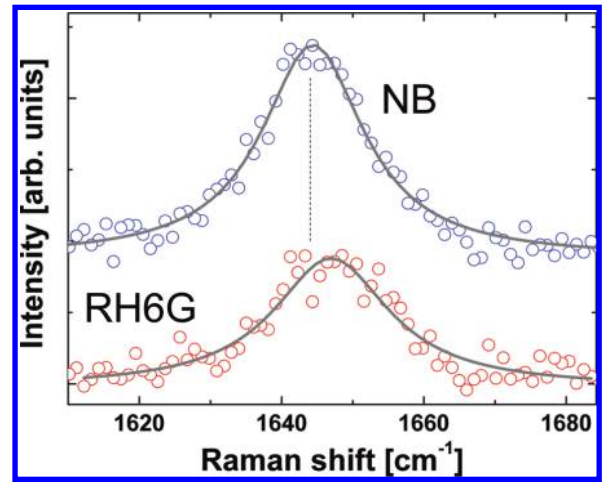

Figure 3. The deconvolution of the spectra works even in regions where there is a substantial overlap of peak intensities for the different compounds. Here we show explicitly the region ~1650 cm^{-1}, where the RH6G peak is deconvoluted from the equivalent ring-breathing mode in NB, which is at a slightly lower frequency.

Consider the case of a mixture of 80 and 20 nM of CV and NB, respectively, as shown in Figure 4(a). The mixture is prepared purposely so that the signal of NB is barely visible in the average spectrum (Figure 1(a)). This is shown explicitly, for example, with the arrows pointing at the ~590 and ~1650 cm^{-1} fingerprint peaks of NB in Figure 4(a), which are almost buried in the immediate surrounding of much larger peaks from CV. Both NB and CV experience (different) electrochemical modulations in the potential range between −50 and −550 mV (the electrochemistry of CV is also summarized in the SI). We can basically follow in a first approximation the analysis performed in the previous section.

With an unlimited amount of sampling, PCA has all what it needs to distinguish the different components in the spectra. This is because the eigenvalues and eigenvectors of the covariance matrix (which is the basis of PCA[41,42]) will eventually distinguish what is correlated and what is random in the signal. For the same reason that unlimited integration time should in principle always lift a signal above the noise level, sufficient sampling will always provide PCA with all the information required to distinguish the different contributions to the spectra. Nevertheless, when big signals are mixed with very small ones from other independent contributions, it is the comparative (with respect to other larger signals in the spectrum) size of the small signals that fix the amount of sampling we need to obtain the principal components from the spectra. This amount of sampling can be, however, prohibitively large. In the case of SERS, for example, photobleaching and other long-term stability problems of the signal puts serious limitation to how much sampling we can obtain. We are left here basically with a conundrum: random fluctuations in large signals with limited sampling might be comparable—as far as contributions to the covariance matrix of PCA is concerned—to the small signals we are trying to modulate and detect on purpose. An example of this is explicitly shown in Figure 4; the region encircled in a box in Figure 4(a) contains a contribution from NB and a much larger peak of CV in the same range. This region is PCA-analyzed and the first four eigenvectors are shown in Figure 4(b). We can see that there is no clear signature of the NB peak in the PCA analysis. The first eigenvector is clearly dominated

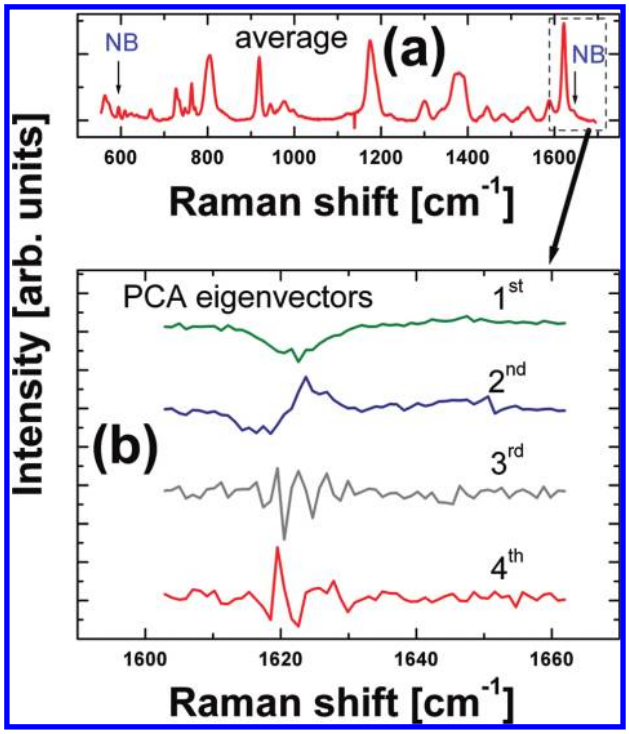

Figure 4. With limited sampling, PCA can have problems to distinguish small components in the spectra. An example is shown here with a mixture of 80 and 20 nM of CV and NB, respectively. In (a) we show the average (over 400 spectra), with arrows showing the positions where the fingerprint modes of NB at 590 cm^{-1} and 1645 cm^{-1} should appear. The signal is dominated by CV throughout the entire spectral range, with many overlap regions. In (b) we show a PCA analysis of the ~1630 cm^{-1} region, where both the 1620 and 1645 cm^{-1} peaks of CV and NB are expected, respectively. But with a difference of factor of ~20 between the intensities of CV and NB in this range, fluctuations larger than ~5% in the CV signal have a larger weight for the covariance matrix than the induced (electrochemical) variations of NB. With limited sampling, PCA cannot clearly distinguish the NB signal. We show here the first four PCA eigenvectors as an example. The limited sampling problem can be partially compensated by a prefiltering of the data with a FFT-transform, filtered at the appropriate electrochemical modulation frequency (see Figure 5).

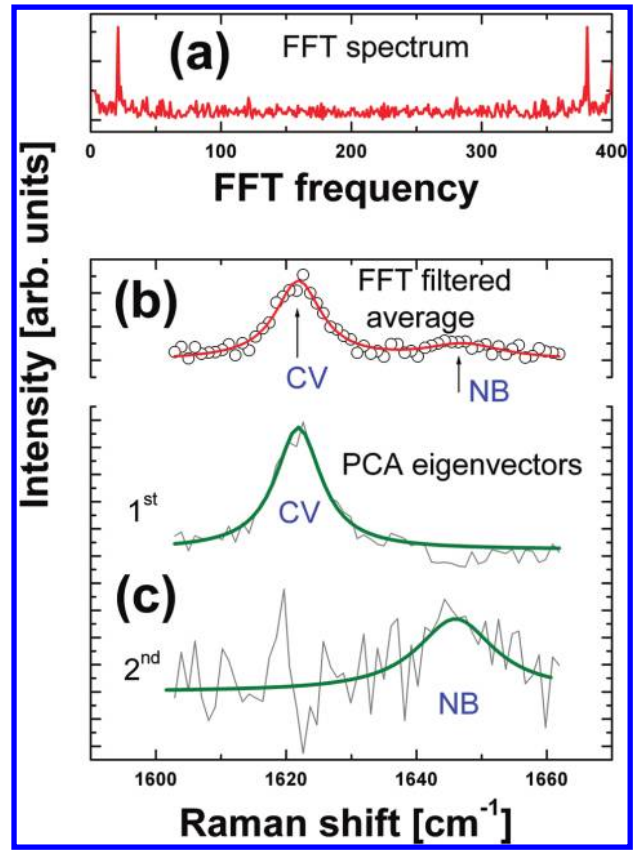

Figure 5. (a) A FFT of the total integrated intensity of the spectra (which varies mainly here due to the electrochemical modulation of CV), reveals clearly the main frequency of the modulation (i.e., scan rate of 50 mV. sec^{-1}). We can filter each pixel (wavelength) at this frequency and then transformed back the spectra into the time domain. The average of the filtered data (at the electrochemical modulation frequency) is shown in (b). Now the signal of NB is more clearly visible in the average and its relative intensity with respect to the CV peak is larger (because only the part of the CV signal that is modulated survives the filtering). A PCA analysis of the prefiltered signal shows a first eigenvector representing the CV intensity, and a second eigenvector which now contains the NB peak at ~1645 cm^{-1}, and a small fraction of frequency shifts of the CV peak. The vertical intensity scale for both curves in (c) is the same. Green lines are guides to the eye.

by the intensity fluctuations of the much larger CV peak, whereas the second one has the typical characteristic of an eigenvector accounting for *frequency shifts* of the CV peak.[40] From the third eigenvector onward, the covariance matrix in PCA is trying to find "correlations in the noise". With enough sampling, these correlations will be zero and the peak of NB will appear as a third eigenvector. But in this case, the limited sampling establishes a competition between the random fluctuations of the much larger peak and the signal we are trying to observe (from NB).

It is in situations like this one that a prefiltering of the data can help. The basic idea of Fourier prefiltering is explained in full in the SI with further examples, but here we shall give a brief version of it. From a FFT-transform of the total integrated intensity as a function of time we can easily reveal the main modulation frequency in the FFT-spectrum, as can be seen in Figure 5(a). This comes primarily from the modulation of the CV signal, but that is irrelevant at this stage: the FFT-transform of the total integrated intensity is used to identify the modulation in FFT-frequency units.[48−50] We can now perform a wavelength-by-wavelength (i.e., pixel-by-pixel) FFT filtering of the data at this particular frequency. This is simply done by an FFT-transform to the time evolution of each pixel, multiplication by an appropriate filter centered at the spikes of Figure 5(a), and followed by an inverse FFT-transform to go back to the time domain. In these data, therefore, we have enhanced the importance of only those fluctuations that happen at the known electrochemical modulation frequency, with respect to any other random fluctuation.

Figure 5(b) and (c) show the resulting PCA analysis after FFT-filtering. It is worth noting that the average of the filtered signal has now a much better ratio of intensities between the CV and NB signals; this is because only the fraction of the CV signal that is being modulated survives the filtering. Accordingly, this puts

(48) Press, W. H.; Flannery, B. P.; Teukolsky, S. A.; Vetterling, W. T. *Numerical Recipes in FORTRAN: The Art of Scientific Computing*; Cambridge University Press: Cambridge, 1989.
(49) Kreyszig, E. *Advanced Engineering Mathematics*, 9th ed.; John Wiley & Sons: New York, 2006.
(50) Kauppinen, J.; Partanen, J. *Fourier Transforms in Spectroscopy*; Wiley-VCH Verlag: Berlin, 2001.

the NB signal in a much better footing to be identified among the first PCA eigenvectors. Effectively, we can see now in Figure 5(c) that the first eigenvector is still dominated by the CV signal, but the second one contains both the NB signal and some contributions to frequency shifts of the CV peak. What we have achieved by FFT-prefiltering is to put the NB signal at the same level of importance of frequency shifts of the CV peak (according to the covariance matrix) and this therefore "lifts" a very small signal from accidental correlations in the noise. As explained further in the SI, this is nothing but the well established principle of "lock-in" amplification; applied here as a prefiltering for PCA. In general, in any other experimental situation, if we have access to unlimited sampling then time lock-in "amplification" might not be needed; for the signal will always increase linearly with time while the noise increases like the square root of it. Therefore, the signal-to-noise ratio will always improve with integration time and eventually a small signal can be resolved. But we can achieve a much faster result in a shorter time (with less sampling) with a lock-in. Like in the case at hand here, unlimited amount of sampling is sometimes not possible in other experimental situations because the long-term stability of the experiment is compromised or it is simply too long. The situation depicted here is the exact analog of this latter situation but for the problem of spectral deconvolution with PCA.

The combination of FFT-prefiltering and PCA might not be necessary in many situations and whenever possible, the simplest analysis should prevail. But the covariance matrix of PCA is basically "blind" to the time sequence of the electrochemical cycle. If we scrambled all the spectra (in time) we would still have the same covariance matrix and the same PCA eigenvectors. However, we *do* know the frequency (or period) with which we are inducing the electrochemical modulation. What we are doing with FFT-prefiltering is, accordingly, to "pick" the appropriate fluctuations that happen at the frequency where we know the real physical effect is happening. In that manner, we bias the PCA analysis toward a physically relevant set of fluctuations, and this helps to improve the ability of PCA to distinguish what is correlated and what is not, in a situation where limited sampling is unavoidable. In the language of lock-in amplification, we have improved the signal-to-noise ratio by discarding all fluctuations except those that happen at the right frequency. The example chosen here is tailor-made to show the concept and, as such, we have different options at hand. We could have done, for example, a PCA analysis is a much narrower window around the NB peak (to try to minimize the influence of the CV peak nearby). However, in real applications, we might not even know where to expect the peaks, and considerable spectral overlap is always possible. FFT-prefiltering is one additional tool to consider in these situation, and it could -in many cases- be the difference between being able to isolate a particular spectral feature of the weaker signal or not.

CONCLUSIONS

We have shown a combination of electrochemical modulation with fluctuation analysis to discriminate and isolate different species in cases where there is spectral congestion and coadsorption of molecules. Needless to say, the technique is not limited to *two* species, and can be applied to multicomponent systems in general. PCA contains, in principle, all the elements it needs to distinguish all spectral components given enough sampling. The restriction of limited sampling to "lift" small signals from other contributions has also been shown through the addition of FFT-prefiltering. Prefiltering is not strange in PCA analysis. The most common type of prefiltering used in the PCA literature is "pre-whitening".[41,42] In this latter case, this is done for a different purpose: to ensure that the samples are as unbiased as possible before the PCA analysis is carried out. Here we use prefiltering in a different way: to bias the study of correlations in the data that happen at a prescribed frequency, imposed externally by the electrochemical modulation. We believe that techniques to solve spectral congestion of coadsorbed species will be of great interest, as SERS moves into areas (like bioelectrochemistry) where the purity and characteristics of the sample cannot be chosen at will. We hope the concepts developed here in our paper will contribute to that endeavor.

ACKNOWLEDGMENT

E.C. acknowledges the financial support of UNLP, ANPCyT (Argentina) and the MacDiarmid Institute (New Zealand) for a research/exchange program between Argentina and New Zealand. Thanks are also given to the host institution, Victoria University of Wellington, where the work was carried out. We acknowledge financial support from ANPCyT (Argentina, PICT06-621, PAE 22711, PICT06-01061, PICT-CNPQ 08-019). E.C., A.F., and RCS are also at CONICET. MEV is a member of the research career of CIC BsAs. R.C.S and A.F. are Guggenheim Foundation Fellows. PGE and ECLR are indebted to the Royal Society of New Zealand for additional financial support under a Marsden Grant.

SUPPORTING INFORMATION AVAILABLE

Additional information and figures. This material is available free of charge via the Internet at http://pubs.acs.org.

Received for review May 3, 2010. Accepted July 10, 2010.

AC101152T